Online ISSN 1848-3380, Print ISSN 0005-1144
ATKAFF 56(4), 395–410(2015)

Joško Deur, Branimir Škugor, Mihael Cipek

Integration of Electric Vehicles into Energy and Transport Systems

DOI 10.7305/automatika.2016.01.1106
UDK 629.03-83:[621.3.05+656.01]-047.58

Original scientific paper

There is a strong tendency of development and application of different types of electric vehicles (EV). This can clearly be beneficial for transport systems in terms of making it more efficient, cleaner, and quieter, as well as for energy systems due to the grid load leveling and renewable energy sources exploitation opportunities. The latter can be achieved only through application of smart EV charging technologies that strongly rely on application of optimization methods. For the development of both EV architectures and controls and charging optimization methods, it is important to gain the knowledge about driving cycle features of a particular EV fleet. To this end, the paper presents an overview of (i) electric vehicle architectures, modeling, and control system optimization and design; (ii) experimental characterization of vehicle fleet behaviors and synthesis of representative driving cycles; and (iii) aggregate-level modeling and charging optimization for EV fleets, with emphasis on freight transport.

Key words: Charging, Driving cycles, Electric vehicles, Fleet, Modelling, Optimization

Integracija električnih vozila u energetske i transportne sustave. U novije vrijeme postoji izražena težnja za razvojem i korištenjem različitih tipova električnih vozila. Ovo može biti korisno sa stanovišta transportnih sustava u smislu omogućavanja efikasnijeg, čišćeg, i tišeg transporta, kao i iz perspektive energetskih sustava zbog dodatnih potencijala za poravnanje opterećenja mreže i iskorištenje obnovljivih izvora energije. Potonje može biti ostvareno samo kroz korištenje tehnologija naprednog punjenja električnih vozila, koje se često temelje na primjeni optimizacijskih postupaka. Za razvoj prikladnih konfiguracija, upravljačkih sustava te metoda pametnog punjenja električnih vozila, potrebno je steći uvid u značajke voznih ciklusa razmatrane flote električnih vozila. Imajući u vidu navedeno, članak predstavlja pregled (i) konfiguracija i modeliranja električnih vozila, te optimiranja i sinteze njihova upravljačkog sustava; (ii) eksperimentalne karakterizacije ponašanja flote vozila i sinteze reprezentativnih voznih ciklusa; te (iii) modeliranja i optimiranja punjenja flote električnih vozila na agregatnom nivou, s naglaskom na teretni transport.

Ključne riječi: punjenje, vozni ciklusi, električna vozila, flota, modeliranje, optimizacija

1 INTRODUCTION

Electric vehicles (EV) represent a key enabling technology to make the transport system more efficient, cleaner, quieter, and less dependent on oil reserves. According to the US Environmental Protection Agency, the transport sector was responsible for 28% of the US greenhouse gas emissions in 2011 [1]. A significant part of these emissions comes from the commercial vehicle sector, which is illustrated by the data pointing that between 16% and 50% of total transport pollutant emissions, and from 20% to 30% of vehicle distance traveled in urban areas, is due to the freight transport activities [2].

Although the fully EVs have zero emissions, the electrified transport can be a viable solution only if the well-wheel emissions are significantly reduced. This means that the electric energy to be stored in EV batteries should mostly come from zero-emission renewable energy sources (RES) such as wind power plants and solar panels [3]. The EV-RES integration is also beneficial from the standpoint of power grid, because the well-scheduled EV charging (e.g. night charging) balances the grid load, it leads to a larger potential of RES energy exploitation during the periods of low grid loads, and can provide grid voltage and frequency regulation services based on vehicle-to-grid (V2G) bidirectional charging technologies [4, 5]. This opens enormous opportunities for development of green integrated transport and energy systems of future, where apart from the substantial individual developments on the EV and RES sides, advanced information and communication technologies (ICT) for EV charging (so-called smart charging) have a key enabling technology role.

Due to the aforementioned emission-reduction significance of freight delivery transport in connection with more stringent regulatory aspects, the related potential for cost reduction (particularly for the urban freight transport), and a less-complex implementation of EV-grid concepts in isolated transport and energy systems, it is believed that proliferation of electrified transport system solutions will dominate in freight delivery sector. Here, there is a need for adapting the freight delivery vehicle routing optimization problem to the electric vehicle constraints (e.g. limited range and required charging period) [2, 6], as well as an ultimate goal of integrating the electric vehicle routing and charging management.

This paper presents an overview of three basic areas relevant for the development of integrated electrified-transport and energy systems: (i) electric vehicles with emphasis on their energy management control system optimization and design, (ii) experimental characterization of driving cycle features and synthesis of naturalistic driving cycles, and (iii) electric vehicle fleet charging optimization. A majority of presentation is based on the research results obtained through the project "*ICT-aided integration of Electric Vehicles into the Energy Systems with a high share of Renewable Energy Sources*" supported by the Croatian Science Foundation. The results of the activities (ii) and (iii) above relate to a freight delivery transport system of the leading regional retail company.

2 ELECTRIC VEHICLES

2.1 EV types and configurations

The EVs can be divided into the following characteristic groups:

1. *Hybrid electric vehicles* (HEV), which combine engine, one or more electric machines, and a battery of a relatively small capacity. The main advantages of HEVs when compared to their conventional counterparts include the possibility of regenerative braking (vehicle kinetic energy is transformed into electric energy and stored in the battery), efficient electric-only driving at low vehicle velocities, and engine operation in highly-efficient operating regions [7-9].

2. *Plug-in electric vehicles* (PHEV), which can be connected to the grid while parked, thus allowing for the possibility of using less expensive and greener energy for propulsion. The PHEV's battery is of a larger capacity than that of a HEV, and the vehicle includes charging and communication hardware and software to provide the grid connection.

3. *Extended range electric vehicles* (EREV), which include stronger electric motor and larger battery capacity than PHEVs, in order to provide electric-only driving under all operating conditions (not only for low velocities). Therefore, the vehicle can be used as purely electric vehicle if the driving distance between two charging events is shorter than the vehicle all-electric range (AER). Otherwise, the vehicle switches from the (electric-only) charge depleting mode (CD) to charge sustaining (CS) mode, in which it operates as a HEV keeping the battery charge around the lower allowed charge limit. Another possibility is to use the so-called blended mode, when the engine is utilized throughout the driving mission for a better efficiency of the overall driving cycle (particularly if the distance is longer than the AER).

4. *Battery electric vehicle* (BEV) or *Fully electric vehicle* (FEV), where only electric energy is used for vehicle propulsion. The battery should have a large capacity for an adequate vehicle range. The electric motor can be connected directly to the driveline, or, alternatively, a gearbox with a low number of gears or a multi-electric machine powertrain can be utilized for improved efficiency at low-speed and/or low-torque operating regimes.

The HEV (and similarly PHEV) powertrain configurations can be divided into three characteristic groups (Fig. 1, [7-10]): parallel, series, and series-parallel configurations. The parallel configuration (Fig. 1b) represents the simplest extension of a conventional powertrain, where the electric motor torque is added to the engine/transmission torque. In the series configuration (Fig. 1a), the internal combustion engine (ICE) is disconnected from the driveline by means of an electric generator and electric motor (an electric shaft), thus providing the possibility of running the engine in its maximum-efficiency region independently of the vehicle velocity (an electric Continuously Variable Transmission feature; e-CVT). The series-parallel configuration (Fig. 1c) utilizes a power split device (typically one or more planetary gears) to transfer a part of the engine power through a mechanical path for improved efficiency, while preserving the e-CVT feature to a large extent. The references [11] describe and analyze the most common series-parallel HEV configurations published in [12-14]. The EREV configurations are usually of series or series-parallel type [15, 16].

2.2 An EREV powertrain configuration

Figure 2 shows the powertrain schematic of the EREV known as Chevrolet Volt or Opel Ampera [16-18]. When the clutch F1 is locked and F2 is open, the planetary gear reduces to a standard two-port gear. If, at the same time, the IC engine is switched off (F3 = OFF), the power train utilizes the main, M/G2 electric machine to propel the vehicle in the EV mode. By switching the engine on (with

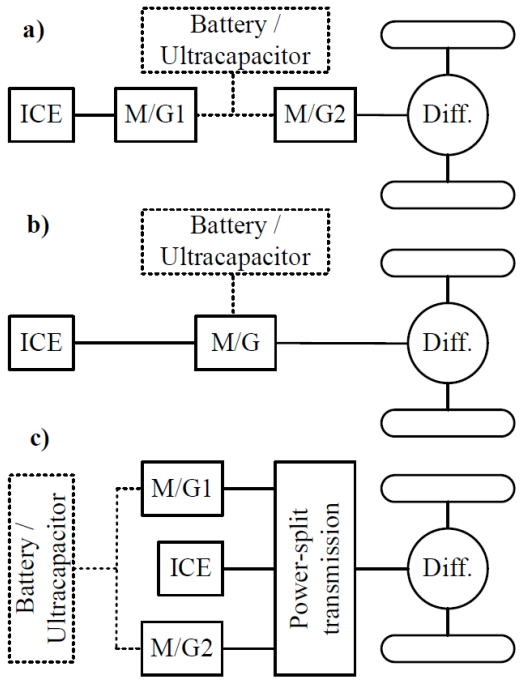

Fig. 1. Basic configurations of hybrid electric powertrains: series (a), parallel (b), and series-parallel configurations (c).

F3 = ON), the powertrain operates in the series HEV mode (SHEV), where the auxiliary electric machine M/G1 generates the energy needed to supply the M/G2 motor and eventually charge the battery. On the other hand, when the clutch F1 is open and F2 is locked, the planetary gear acts as a power split device, which transfers a part of the engine power through the mechanical path in the series-parallel HEV mode (SPHEV). Finally, if the engine is switched off, the power split feature enables the two electric motors to propel the vehicle (two motor EV mode, TMEV).

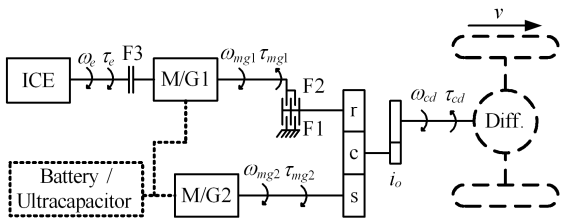

Fig. 2. Principal schematic of an EREV powertrain [17, 18].

2.3 Control-oriented modeling

For the purpose of energy management control strategy design, an EV powertrain is usually described by a backward-looking mathematical model [10]. Such a model assumes that the vehicle velocity v (i.e. the transmission output speed ω_{cd}, Fig. 2) and the road load (i.e. the transmission output torque τ_{cd}) inputs are known from the driving cycle specification and the road load model, respectively. They are then used together with the control variables (here, ω_{mg1} and τ_e, as well as the operating mode variable $s_{mode} \in \{1, ..., 4\}$) to calculate the engine and electric machine speed and torque variables (Fig. 3). The calculation is based on the transmission kinematics model [18, 19], given by the equations included in Table 1. The engine torque is limited based on the maximum torque map, and another map is used to calculate the fuel mass flow dm_f/dt. Similarly, the electric machine torque limit and efficiency maps are used to limit their torques and determine their electric powers used as inputs to the battery model.

The battery state-of-charge (*SoC*) is only state variable of the backward vehicle model, and its dynamics are described as [20]

$$\dot{SoC} = \frac{\sqrt{U_{oc}^2(SoC) - 4R(SoC,i)P_{batt}} - U_{oc}(SoC)}{2Q_{\max}R(SoC,i)}. \tag{1}$$

Here, U_{oc} denotes the battery open circuit voltage, R is its internal resistance, P_{batt} is the battery power determined from the M/G1 and M/G2 machine electric power values (Fig. 3), and $Q_{\max}$ is the battery capacity, where $0 \leq SoC = Q/Q_{\max} \leq 1$.

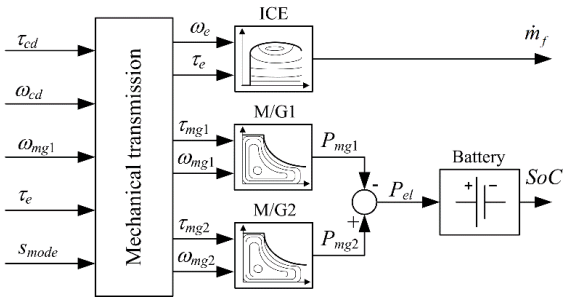

Fig. 3. Block diagram of backward-looking model of EREV powertrain.

2.4 Control variable optimization

The optimization problem is to find optimal open-loop time responses of the transmission machines' torque and speed control variables and the control mode variable,

Table 1. Transmission steady-state equations for different operating modes (i_o = final drive ratio and h = planetary gear ratio) [18].

MODE	ω_{cd}	τ_{cd}
EV, SHEV	$\frac{1}{i_o(h+1)}\omega_{mg2}$	$i_o\,(h+1)\,\tau_{mg2}$
SPHEV,TMEV	$\frac{1}{i_o(h+1)}\,(\omega_{mg2}+h\omega_{mg1})$	$i_o\,(h+1)\,\tau_{mg2} =$ $i_o\,(h+1)\,h^{-1}\,(\tau_e-\tau_{mg1})$
MODE	ω_e	τ_e
EV	0	0
SHEV	ω_{mg1}	τ_{mg1}
SPHEV	ω_{mg1}	$h\tau_{mg2}+\tau_{mg1}$
TMEV	0	0

which minimize the fuel and/or electric energy consumption, while satisfying battery state of charge (SoC) constraints and physical limits of the transmission variables. The optimization is usually carried out by using the dynamic programming (DP) algorithm, because it provides the global optimum solution [10, 21]. The optimization results are used for the purpose of design and assessment of realistic (closed-loop) control strategies (see the next subsection).

Figures 4b,c show the charge sustaining (CS) mode optimization results for the EREV powertrain shown in Fig. 2 and modeled in Fig. 3, where the "aggressive" US06 driving cycle is considered (Fig. 4a) and the aim is to minimize the fuel consumption m_f at the end of driving cycle [21]. The optimization results plotted in the powertrain output map (Fig. 4b) clearly indicate distinct areas of optimal vehicle operating points for the four driving modes in the CS regime. For low-mid vehicle velocities and high traction torque (abrupt accelerations/decelerations) the vehicle mostly operates in the EV mode. For high velocities and still high traction torques (i.e. for the high traction power), the transmission switches to the SHEV operating mode, in order to reduce high electricity consumption from the battery to satisfy the charge sustaining condition. The power split modes (TMEV and SPHEV) have their operating points mostly located in the areas of mid-high velocities and low-mid torques, where the TMEV mode operating points are shifted deeper in the low-torque region. In this area, the TMEV mode has better efficiency than the EV mode, and the SPHEV mode is more efficient than the SHEV mode. The electric-driving EV and TMEV modes are exploited during (regenerative) braking intervals ($\tau_{cd} < 0$).

The engine map-related optimization results (Fig. 4c) indicate that the majority of engine operating points are located inside or near the area of highest engine efficiency, which are nearby or slightly below the maximum engine torque curve.

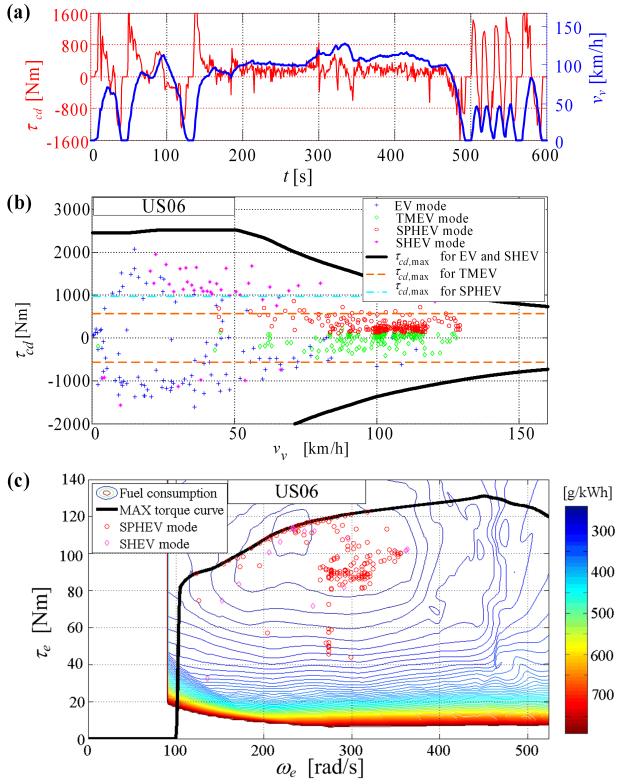

Fig. 4. EREV optimization results (b, c) for US06 driving cycle (a) and CS mode.

If the vehicle driving range is known in advance and if it exceeds the AER, the battery could be discharged more gradually by combining all operating modes during the whole driving cycle [22]. This leads to the blended operating regime (BLND) as opposed to the CD-CS regime. Figure 5 shows the comparative, BLND vs. CD-CS DP optimization results for the case of several repetitive certification driving cycles [19]. In the considered scenario of

approximately 50:50 CD/CS duration ratio, the benefits of BLND operation have been found to be the most emphasized. The fuel consumption (m_f) reduction when using the BLND mode ranges from approximately 2.5% to more often closer to 5%, depending on the type of driving cycle. The optimization results also indicate that the optimal state-of-charge (SoC) trajectory during the blended mode have a linear (ramp) shape for the considered case of zero road grade (see also [23]).

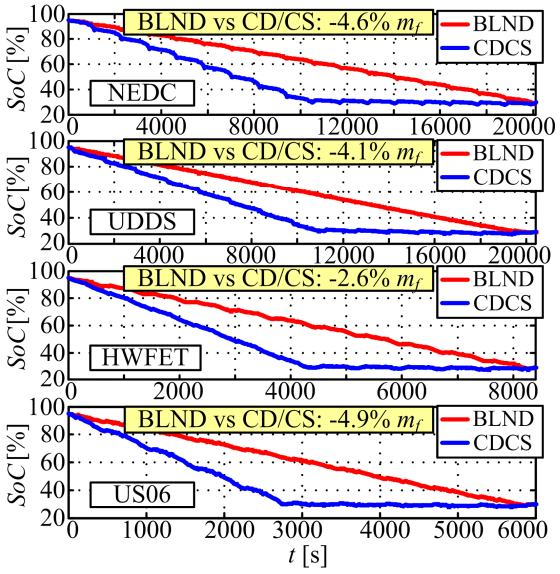

Fig. 5. BLND vs. CD-CS regime optimization results for NEDC, HWFET, UDDS and US06 repetitive driving cycles.

2.5 Energy management control strategy

The aim of an energy management control (EMC) strategy is to provide on-line updates of control variables (i.e. ω_{mg1}, τ_e, and s_{mode} for the particular case of EREV, Fig. 3) based on the driver commands and the actual SoC estimate [10]. These control variables are realized on a shorter/faster time scale by means of a low-level controller, which switches clutches, executes closed-loop control of the generator speed and commands the engine throttle [24, 25, 31].

In applications, the EMC strategies are typically of rule-based type including SoC feedback control [26, 27]. On the other hand, many research papers deal with design of strategies based on instantaneous minimization of fuel consumption (so-called Equivalent Consumption Minimization Strategy, ECMS; [10, 28, 29, 30]). The equivalent fuel consumption to be minimized consists of real fuel consumption and the "virtual" fuel consumption related to the actual battery power since the battery energy was obtained from the fuel in the past (if the hybrid/CS mode is considered).

The references [31, 32] propose to combine the rule-based and ECMS approaches to benefit from their complementary advantages in terms of robustness and favorable fuel economy, respectively. Such an EMC strategy is outlined by the block diagram shown in Fig. 6, which can be directly applied to an HEV [31]. The driver's power command (P_d) is combined with the battery power demand (P_{batt}), obtained by a SoC feedback controller, in order to calculate the engine power demandP_e^*. If the engine power demand P_e^* is lower than the lower threshold P_{off}, the engine is switched off for electric-only driving, and when the demand P_e^* exceeds the upper threshold P_{on} the engine is again switched on. For the active engine, the engine power demand P_e^* at the same time represents an input to an ECMS algorithm, which smoothly combines an 1D search over the constant engine power line of the τ_e vs. ω_e engine map and a 2D search of a pre-optimized area of the same engine map. In this way, it finds the control variables τ_e and $\omega_e = \omega_{mg1}$.

In the EREV case, the EMC strategy additionally includes an algorithm that determines the operating mode based on the distinct mode-boundary curves obtained from the control variable optimization results (Fig. 4b) [32]. The control strategy from Fig. 6 is applied for the hybrid-driving SHEV and SPHEV modes.

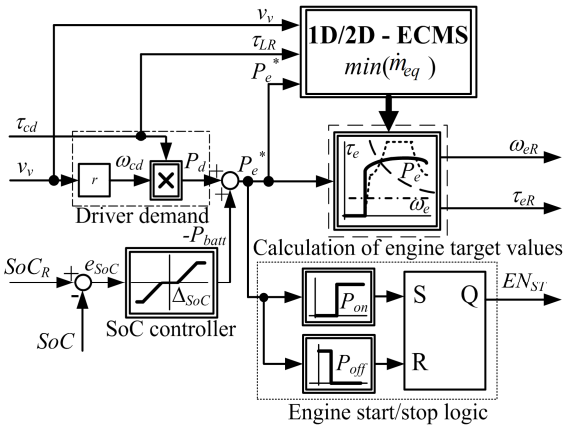

Fig. 6. Block diagram of energy management control strategy for hybrid modes.

Figure 7 shows the EREV control strategy verification results in comparison with the DP global optimum benchmark, where the CS regime and New European Driving Cycle (NEDC) are concerned. Compared to the purely rule-based strategy (RB), the final, combined 1D and 2D ECMS-based strategy provides a significant reduction of

the fuel economy. Namely, it approaches the global optimum benchmark with the margin of 2.3% for the particular case of NEDC, while this margin equals 1.1% and 4.5% for the UDDS and HWET driving cycles, respectively [32]. This is considered to be a favorable result, taking into account that, unlike the real control strategy, the DP optimization is conducted over the full driving cycle horizon and can switch the engine on/off at any instant. More detailed verification results, including those related to the BLND regime, are given in [19, 32].

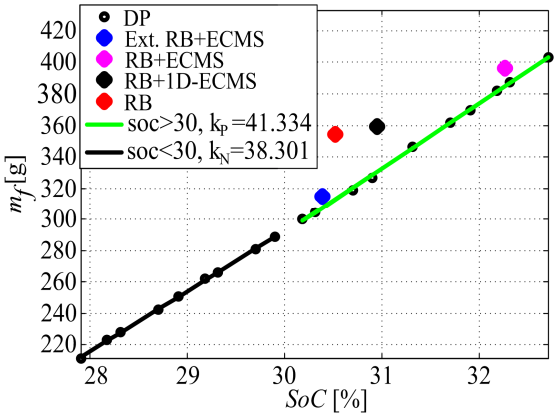

Fig. 7. EREV control strategy verification results with respect to DP global optimum results (CS mode and NEDC).

3 EXPERIMENTAL CHARACTERIZATION OF FREIGHT TRANSPORT SYSTEM AND E-TRUCK DESIGN

A target transport system including a fleet of conventional vehicles should first be characterized (see e.g. a passenger vehicle study in [33]), as a basis for fleet electrification and analysis of its competitiveness. This section presents the experimental characterization results related to a city and intercity freight transport system of the regional retail company, Konzum d.d. It also presents design of a fully electric truck powertrain, as well as its assessment in terms of efficiency, energy cost and CO2 emissions.

3.1 Subsection data collection and analysis

The data have been recorded for a representative fleet sample of ten 7.5 ton delivery vehicles equipped with GPS/GPRS system, and three-month period of continuous 24 hour operation. The main recorded signals include the vehicle velocity (with the resolution of 0.1 km/h), absolute vehicle position, and cumulative fuel consumption, all acquired with the sampling time of 1 sec. The vehicles are loaded in the main distribution center, unloaded in one or more sale centers, and driven back to the distribution center to complete a driving mission (cycle). Figure 8 shows the vehicle trajectory and the vehicle velocity response during an intercity mission, as an illustration of recording quality.

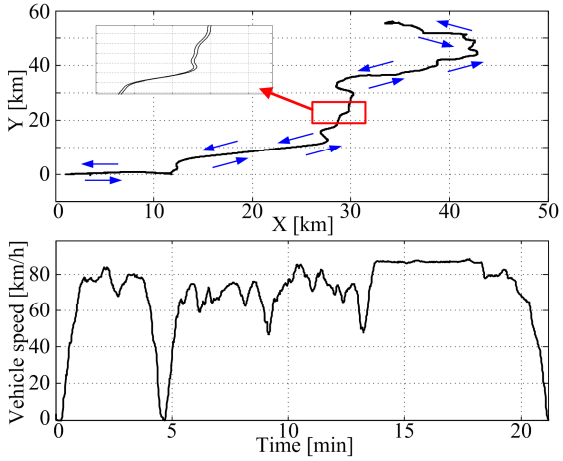

Fig. 8. Recorded data for an intercity driving mission.

The recorded large set of data has been processed for the purpose of various statistical analyses. These analyses are mostly related to vehicle arrival, departure, and resting time features for the main distribution center and different sale centers, because they correspond to vehicle charging availability if a hypothetical electrified fleet is considered. The main results are presented in the remaining part of this subsection, while a more detailed presentation and analysis can be found in [34, 35].

Figure 9 shows the vehicles arrival and departure time distributions for the distribution center, which demonstrates the 24h fleet activity. Vehicles departure time distribution peaks are emphasized around 7h, 15h, and 21h. While the arrival time distribution has roughly similar shape as the departure time distribution, the departure times are apparently delayed by around five hours during the night pause and by one to two hours, otherwise. These delays are indicators of vehicle/fleet resting times and, correspondingly readiness for charging: slow and cheap charging overnight and fast and more expensive charging over day or early night.

Indeed, the distribution center resting time distribution, shown in Fig. 10a, indicates that a majority of resting durations is less than two hours (mostly around 50-60 minutes), while another significant peak of resting time distribution is around 6 hours. In the case of sale centers, the peak of resting time distribution is around 20-30 minutes, the distribution diminishes already at 50-60 min, and there are no resting time durations longer than 1 hour (Fig. 10b).

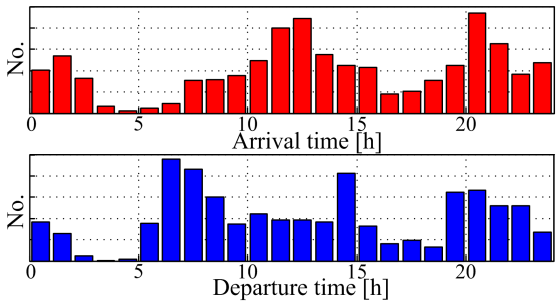

Fig. 9. Arrival and departure time distributions for main distribution center.

Therefore, only the fast charging could be implemented in sale centers.

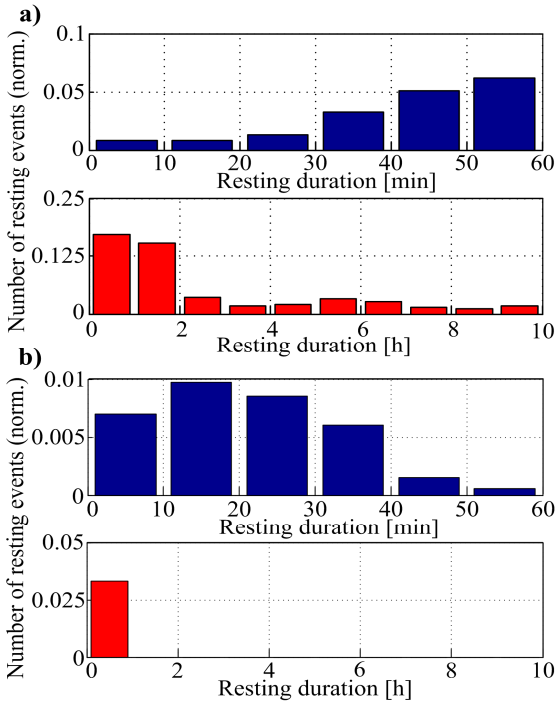

Fig. 10. Resting time distribution for main distribution center (a) and one of sale centers (b).

The traveled distance distribution for the full set of driving missions is another important feature of the fleet, because it can indicate an adequate type of electric vehicle and sizing of its components. As shown in Fig. 11, a majority of the traveled distances (around 60%) for the given fleet are within 100 km range. These missions could be covered by using purely electric delivery vehicles, even without fast charging in the sale centers. The remaining 40% of missions could be covered by extended range or (plug-in) hybrid electric vehicles.

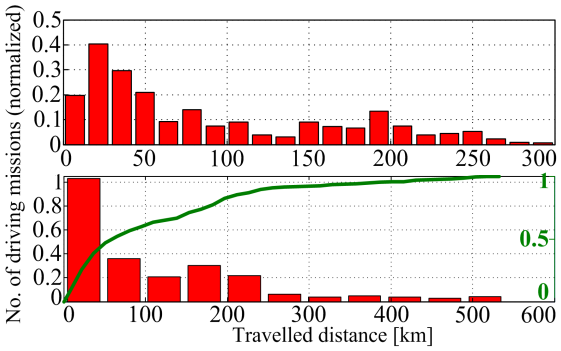

Fig. 11. Traveled distance distribution.

The time distribution of transport system energy consumption can be estimated by inverting the time distribution of number of parked vehicles. Such a distribution, shown in Fig. 12a for the main distribution center, indicates that the time distribution of average number of parked vehicles is repeatable for work days, while it tends to be saturated over the weekend (a large number of vehicles are parked). Figure 12b shows the daily-averaged ("lumped") time distributions of the number of vehicles parked in the distribution center, sale centers, and both distribution and sale centers. The total/overall distribution is then inverted and normalized to reflect the average fuel consumption (of on-road vehicles; see the blue plot in Fig. 12c). The red plot in the same figure shows the actual average fuel consumption, which has been obtained from the vehicle online recorded data. A relatively good correlation between the two traces in Fig. 12c indicates that the transport system energy consumption may be estimated based on the vehicle on-road activity, in the absence of more precise source of data.

Figs. 12a,b also illustrate that the vehicles are largely available for charging during the night hours and weekend when the electric energy is cheap and when charging would effectively level the grid load. Also, a large charging availability during the afternoon hours can be exploited in terms of using the electric energy produced by photovoltaic panels mounted on the distribution center roofs.

3.2 Synthesis of naturalistic driving cycles

The aim of naturalistic driving cycles synthesis is to replace a large set of actual (recorded) driving cycles with several synthetic, statistically representative cycles, which can be employed for design and verification of EV control strategies [36] instead of usually used "artificial" certification driving cycles such as NEDC. The synthesis is based on discrete Markov chains probability methodology [33].

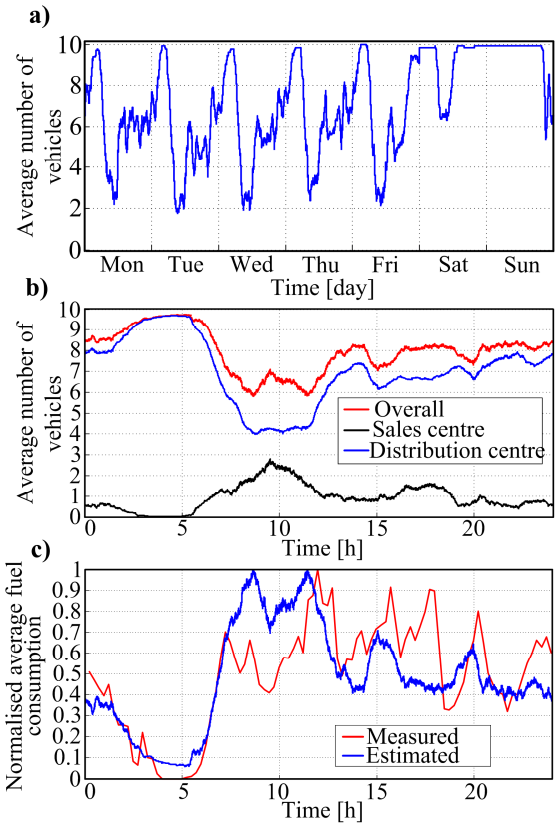

Fig. 12. Averaged weekly and daily distributions of number of parked vehicles (a, b), and related normalized measured and estimated fuel consumptions (c).

The synthesis procedure can be divided into three main steps [33]: (i) clustering of recorded driving cycles, (ii) determination of transition probability matrix (stochastic modeling), and (iii) generation and validation of synthetic driving cycles (stochastic simulation).

The aim of clustering the recorded driving cycles is to separate recorded cycles into several characteristic groups according to predefined criteria and to model these groups separately. Assuming that the vehicle traveled distance is the clustering criterion and applying the "k-means" clustering algorithm yields the clustering results shown in Fig. 13 [34, 35]. The legend of the same figure includes the cycle duration median values for each cluster, which will be used as input parameters of the synthetic driving cycle generation.

In the case of considering only the vehicle velocity v as the Markov chain state, the transition probability matrix elements p_{ij} denote the probability of transition from the velocity state v_i at a time step k to the velocity state $v_j$at the next, $(k+1)^{th}$ time step. Figure 14 shows the results in the form of contour plot, which indicate that the velocity transition probability plot is wider at lower velocities, because the vehicle accelerations are then generally higher.

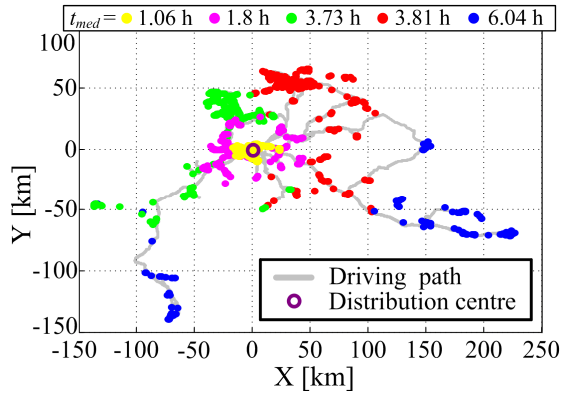

Fig. 13. Recording driving cycle clustering results.

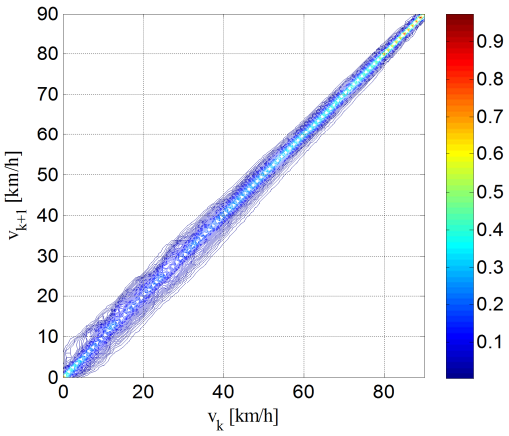

Fig. 14. Transition probability matrix values for 3rd cluster from Fig. 13.

The transition probability matrix and a generator of random numbers are used to synthesize driving cycles. The synthesis procedure is described in [34, 35] and applied to two characteristic cases: (i) the vehicle velocity v is the only Markov chain state, and (ii) the states are vehicle velocity v and acceleration a.

Since the driving cycle synthesis procedure is based on stochastic modeling and generation, many synthetic cycles of different statistical features can be generated by using the same transition probability matrix. In order to select representative synthetic driving cycles, a number of generated cycles should be validated with respect to significant statistical parameters such as mean velocity, mean positive acceleration, and mean negative acceleration, and

related standard deviations [33]. The normalized distributions of these statistical parameters for the case of 2375 individual recorded driving cycles of variable duration are shown in Fig. 15 (the legend label 'Rec'). The same figure includes the values of statistical parameters for a single, combined driving cycle including concatenated individual recorded driving cycles (the legend label 'Comb'). Finally, the figure shows the normalized distributions of statistical parameters for 1000 generated one-state (Syn_1) and two-state (Syn_2) synthetic driving cycles. Evidently, the two-state method gives more representative synthetic driving cycles, because the distribution of their statistical parameters is narrower and centered around the combined recorded cycle statistical parameters [35].

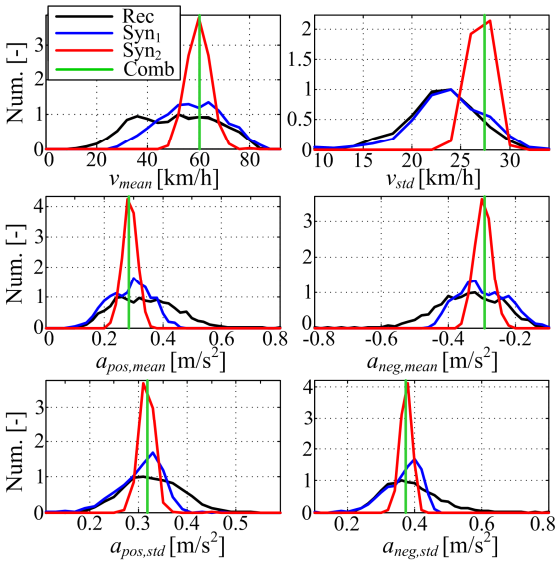

Fig. 15. Synthetic driving cycle validation results.

The selected synthetic driving cycles obtained by the two-state method are shown in Fig. 16 for different clusters from Fig. 13 (the cycle data can be downloaded through the web link [37]). It can be observed that the synthesized driving cycles in the first two subplots of Fig. 13 are more city driving-like cycles, while the other synthesized driving cycles (particularly the last one) include properties of highway driving, which is in a direct correlation with the corresponding clustering results shown in Fig. 13. If the one-state synthesis method were used, the generated cycles would be smoother and in worse correlation with the recorded cycles [35].

3.3 Design and assessment of fully-electric delivery truck

The above-considered conventional truck (MAN - TGM 15.240) has the loading capacity of 7460 kg and the

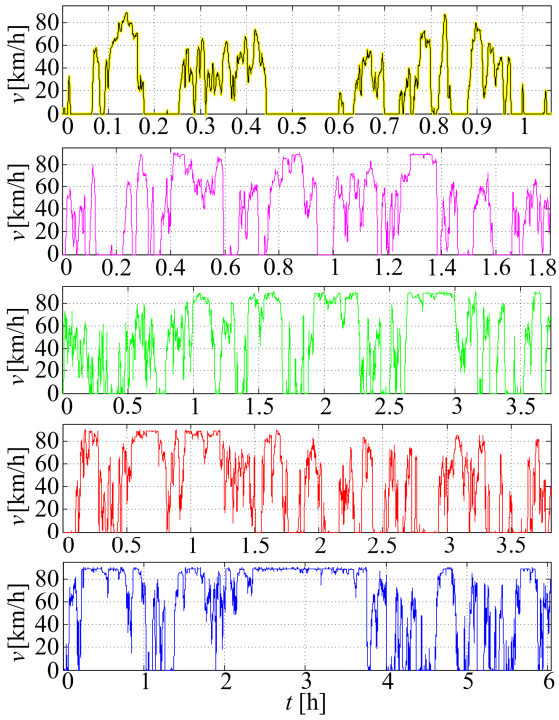

Fig. 16. Selected synthetic driving cycles for each cluster of recorded driving cycles.

empty-vehicle mass of 7860 kg. The vehicle velocity is limited to 90 km/h. The vehicle is propelled by a diesel engine with the maximum power of 176 kW. The engine is described by the specific fuel consumption and maximum output torque maps shown in Fig. 17a and taken from [38, 39] based on a similar diesel engine. By using the catalogue data for the 12-speed automated manual transmission and differential gear ratios [39], the powertrain output torque vs. vehicle velocity map can be reconstructed, as shown in Fig. 17b.

By using the maps in Fig. 17 and known and estimated basic truck parameters (such as mass, tire radius, aerodynamic drag and tire rolling coefficients, and drivetrain efficiency), the truck longitudinal dynamics model has been developed in [40]. The model has been validated with respect to recorded fuel consumption data for different recorded driving cycles. The validation results point out that the model-predicted fuel consumption differs from the recorded one by less than 10% for a great majority of driving cycles, thus confirming an acceptable modeling accuracy [40].

For an e-truck model, an electric motor with the rated power of 128 kW and the overload capability of 280 kW [42] has been selected in conjunction with a two-speed gearbox (with the gear ratios h_{t1} = 8.203 and h_{t2} = 3.733).

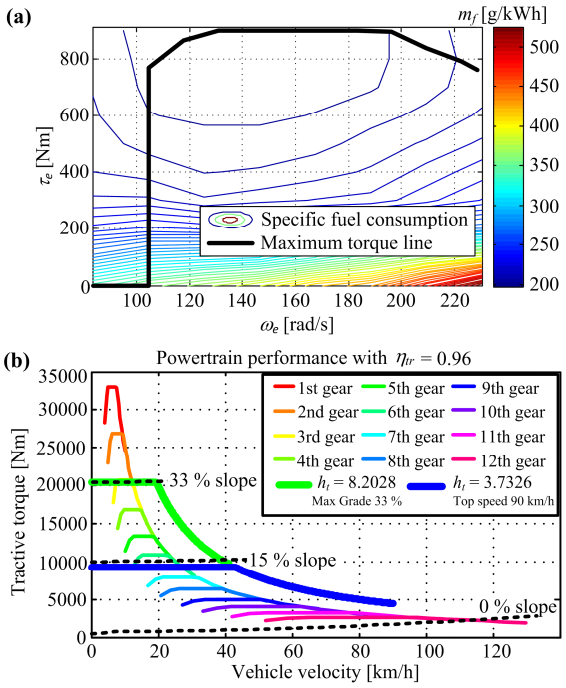

Fig. 17. Delivery truck diesel engine maps (a) and comparative torque limit curves for conventional and electric truck drivetrains (b).

Figure 17b illustrates that this powertrain satisfies or exceeds the required conventional truck maximum torque curve specifications, including the velocity limit of 90 km/h and the maximum road grade of 33%.

Figure 18 shows the comparative energy consumption, energy cost, and CO2 emission plots for the conventional and electric trucks, based on the assumption of constant velocity driving and the total efficiency of battery and charger of 80% [40, 41]. The following local fuel and two-tariff electricity costs were taken into account: Diesel = 1.313 euro/liter; low-tariff electric energy EE-LT = 0.06 euro/kWh; high-tariff electric energy EE-HT = 0.13 euro/kWh. The well-to-wheel CO2 emissions were considered, where it was assumed that one liter of diesel fuel produce 3.16 kg CO2, while the electricity, depending on technology, can emit around 1 kg CO2/kWh for coal fired power plants, 0.45 kg CO2/kWh for natural gas power plants and 0.1 kg CO2/kWh for nuclear energy and renewable sources [41]. Evidently, the e-truck is significantly more efficient than its conventional counterpart, particularly at lower velocities (Fig. 18a). Furthermore, the energy costs can be up to five times lower for the e-truck if the low-tariff overnight-charging is considered. Finally, the e-truck can give significant CO2 reduction benefits, but only if the electricity is generated from renewable energy sources.

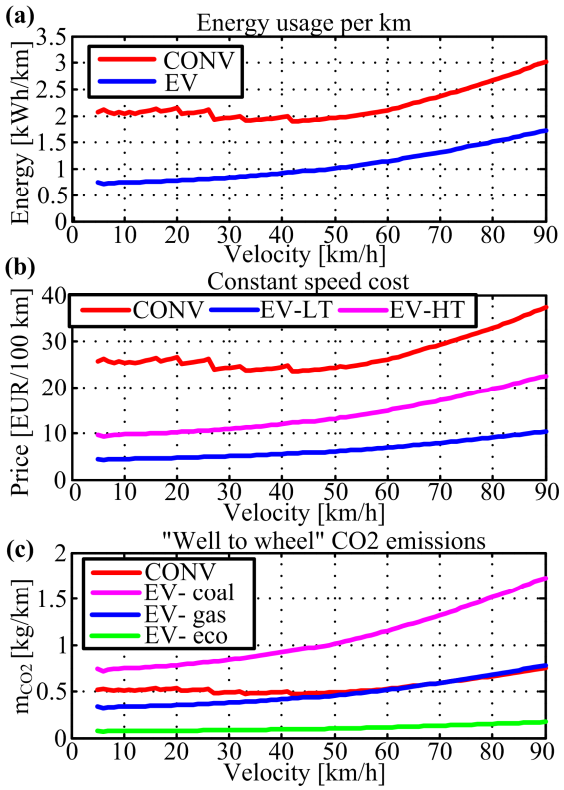

Fig. 18. Comparative specific energy consumption (a), energy cost (b), and well-to-wheel CO2 emission plots (c) for the conventional and electric trucks.

Based on the preliminary constant-velocity analysis and the requirement to satisfy the city cluster range ($\approx$ 70km) for the maximum payload, a 114 kWh Li-Ion battery has been selected. The battery mass of 1.2 t approximately replaces the diesel engine, automatic transmission and fuel tank mass. In order to verify the driving range for realistic driving scenarios, a simulation analysis has been conducted for two certified driving cycles (heavy duty NEDC and UDDS), and also for five synthetic driving cycles (SYN1-SYN5) from Fig. 16. The simulation results shown in Fig. 19 indicate that for the selected battery and the urban and near-urban driving cycles (UDDS, NEDC, SYN1, and SYN2) the electric vehicle range is from 60 to 105 km depending mostly on the cargo load.

4 EV FLEET AGGREGATE BATTERY MODELING AND CHARGING OPTIMIZATION

The main aim is to optimize the charging power time-response for individual EVs from a fleet, which would satisfy the vehicle routing schedule and at the same time minimize the cost of electricity for the given grid and charging

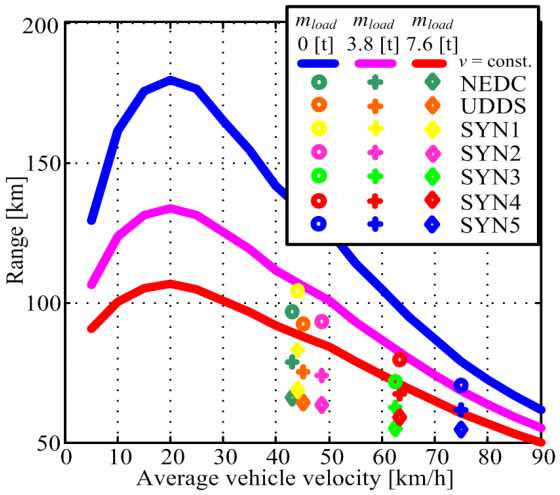

Fig. 19. Predicted range of e-truck for constant velocity driving and various certified and synthesized naturalistic driving cycles.

station constraints [5]. Although the problem can be attacked from different perspectives [3, 43, 44, 45, 46], it appears that the most systematic and effective way is to use a hierarchical charging management system [45-47]. In such a system, the charging is first optimized on the EV fleet aggregate level, and the lumped charging-power request is then distributed (allocated) to the individual EVs. The individual power requests are finally commanded to low-level charging controllers, which execute those commands and at the same time they can provide the ancillary grid services, such as grid stabilization [48, 49] and reactive power compensation [50-52]. Evidently, the charging optimization and control at the different levels of the hierarchical structure are coupled through various grid/charger constraints. It should be noted that the aggregate-level charging optimization has also direct application to various energy planning studies related to EV-grid integration (see e.g. [3]).

4.1 Modeling of EV fleet aggregate battery

For the aggregate-level charging optimization, an aggregate battery model is required. Here, the whole set of EV fleet batteries is replaced by a single, aggregate battery with a single state variable representing the lumped state of charge (SoC_{agg}) and a single charging power input ($P_{c,agg}$).

By following [3], a basic aggregate battery model can be created based on the following input time-distributions: (i) number of vehicles connected to the grid (n_{dc}), (ii) aggregate fleet driving power demand ($P_{dem,agg}$), and (iii) aggregate fleet regenerative braking charging power. The distribution n_{dc} is required only to provide the charging power upper limit: $P_{c,agg} \leq n_{dc} P_{c\,\max,ind}$, where $P_{c\,\max,ind}$ is the maximum charging power of individual vehicle/battery.

The basic model assumes constant battery capacity available for charging at all times, which is found unrealistic since a part of vehicles within the fleet will be driving and thus disconnected from the grid. Also, the aggregate battery SoC limit should be made time-variant depending on the number of vehicles connected to the grid, in order to provide realistic conditions for charging. This has motivated the development of a novel aggregate battery model presented in [53].

The discrete-time state equation of the novel aggregate battery model, formulated in the energy instead of charge domain, is given by:

$$SoC_{agg}(k+1) = SoC_{agg}(k) + SoC_{in,avg}(k)\frac{\Delta n_{in,dc}(k)}{N_v} - SoC_{out,avg}\frac{\Delta n_{out,dc}(k)}{N_v} + \eta_{ch}\frac{P_{c,agg}(k)\Delta T}{E_{\max,agg}} \quad (2)$$

The model requires the knowledge of the following input time distributions (in addition to $n_{dc}(k)$): (i) the number of vehicles connecting to ($\Delta n_{in,dc}$) and disconnecting from the grid ($\Delta n_{out,dc}$) in each time step ΔT, and (ii) the average SoC of vehicles connecting to the grid ($SoC_{in,avg}$). The average SoC of vehicles disconnecting from the grid ($SoC_{out,avg}$) may be regarded as a control parameter, which may be set to 1 in many cases (assuming that the departing vehicles have fully charged batteries). The meaning of other quantities in Eq. (2) are as follows: $k = 1, 2, ..., N_t$ is the discrete time step, N_v and N_t are the number of vehicles and time steps, $E_{\max,agg}$ is the aggregate battery maximum energy capacity, and η_{ch} is the charging efficiency. The upper constraint on SoC_{agg} can readily be made variant in dependence on the number of vehicles connected to a grid: $SoC_{agg}(k) \leq n_{dc}(k)/N_v$. The transport demand is accounted for through the distribution of average SoC of vehicles connecting to the grid ($SoC_{in,avg}$).

In the particular case study related to the delivery vehicle fleet (Section 3), the input distributions related to the number of vehicles are reconstructed from the full set of recorded driving cycles. The transport demand-related distributions (including the SoC at arrival) are obtained through simulation of individual vehicle behaviors over the full set of driving cycles. The details of input distribution reconstruction and results are given in [53].

The optimal charging power input$P_{c,agg}$, for both basic and novel model, is obtained by using a dynamic programming-based optimization algorithm aimed at minimizing the electricity cost (Subsection 4.2). Optimized

daily charging power and aggregate battery SoC profiles are shown in Fig. 20 for the case of a two-tariff electricity price model, along with the realistic SoC and charging power constraints. It can be noticed that the SoC upper limit is frequently violated for the basic model, while it is largely satisfied for the novel model.

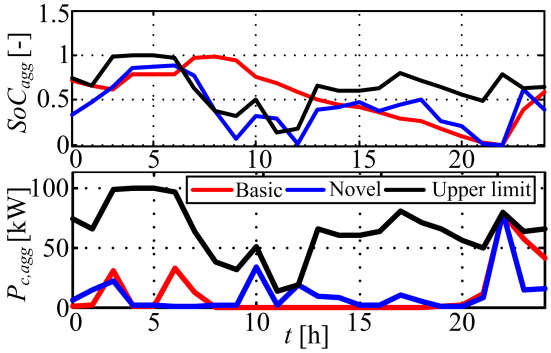

Fig. 20. DP optimized aggregate battery SoC and charging power daily time profiles for basic and novel aggregate battery models.

To facilitate further comparison of the two aggregate battery models, a heuristic iterative algorithm for distributing the optimized aggregate charging power input to the individual vehicles has been proposed in [53]. The level of correlation between the original (optimized) and achieved (through distribution) aggregate SoC and aggregate charging power profiles indicates how well an aggregate model represents the distributed model. The level of correlation is assessed by means of the correlation index [54], which is applied to the input signal vectors **x** and **y** and has a higher value for better correlation (ideally,$K_{x,y} = 1$ for **x** = **y**). Figure 21 indicates that the novel model is consistently superior to the basic one in terms of higher SoC and charging power correlation coefficients K_{SoC} and K_E, respectively. Also, when using the novel model, a lower discrepancy of fleet charging cost (C_{agg}) in comparison with distributed model cost (C_{real}) is observed.

4.2 EV fleet charging optimization

The EV fleet transport system, integrated into the power grid including (local) renewable energy sources (RES), has a similar aggregate-level power flow structure as a hybrid electric vehicle (see illustration in Fig. 22). Namely, both systems include a power source (grid or engine), a battery (aggregated or individual), and a power demand including transport demand. Therefore, the DP optimization method applied in Section 2 to hybrid vehicles can conveniently be applied to the EV fleet aggregate charging system. Such an approach, which provides the

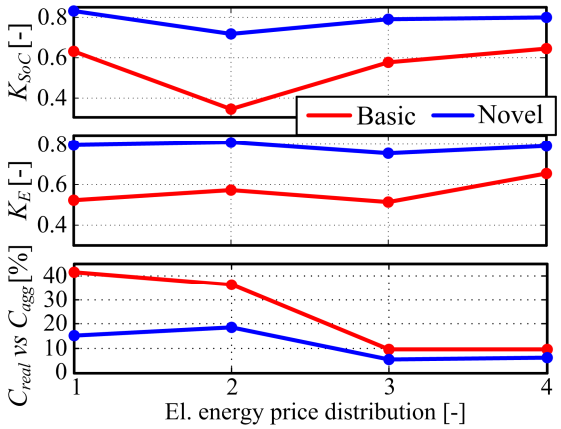

Fig. 21. Correlation factors describing accuracy of basic and novel aggregate battery models for different electricity price models [53].

global optimum solution for a general nonlinear system with nonlinear constraints, is proposed in [46] as opposed to heuristic charging methods such as the one presented in [3].

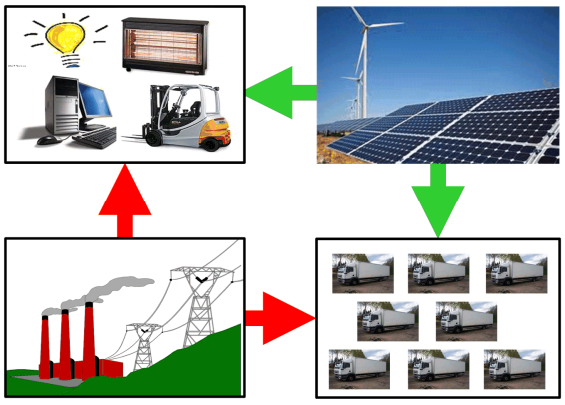

Fig. 22. Illustration of power flow in electrified freight transport system.

In order to demonstrate the DP optimization approach, the simpler, basic model of EV fleet aggregate battery is used and parameterized with respect to recorded driving cycles of the delivery vehicle fleet (see Subsection 4.1 and [53]). The hourly distribution of grid power consumption in the distribution center is estimated from the full-year daily consumption data. A hypothetical electrical energy production from photovoltaic sources is estimated based on a sun global horizontal irradiance time-distribution at the given distribution center location. Details of modeling the transport and energy system are given in [46].

The charging optimization has been conducted for two scenarios of RES energy production: without and with RES energy production excess with respect to demand other than the transport one. The optimization results are shown in Fig. 23 for the case of two-tariff electricity price model. In the case of no RES energy production excess (Fig. 23a), the DP optimizer mostly charges the battery in the periods when the price of energy is low (night charging). Consequently, it provides significant savings in terms of electricity prices, which range from 10% to 40% depending on the electricity price model [46]. Furthermore, the DP algorithm provides that the charge sustaining condition is satisfied (final SoC is equal to the initial SoC), as opposed to the heuristic algorithm which results in a gradual depletion of battery (Fig. 23a).

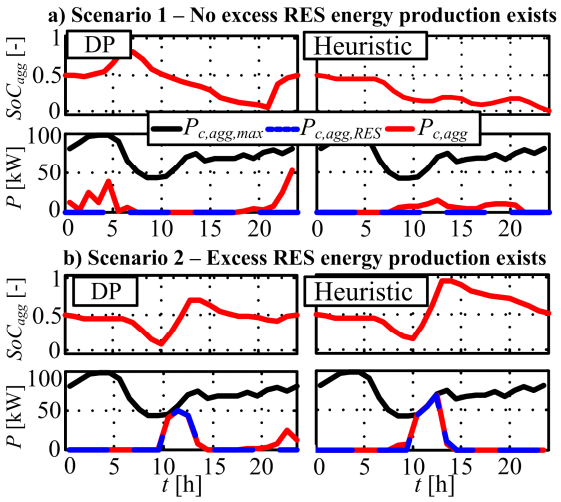

Fig. 23. Aggregate battery charging results using DP optimization and heuristic approaches for two RES energy production scenarios.

In the second scenario, both DP and heuristic algorithms result in charging the battery around solar noon when the excessive energy production from photovoltaic RES exists (Fig. 23b). This is an expected result having in mind that the heuristic method was designed with the main aim of employing the RES potential [3].

4.3 Integrated optimization of EV routing and charging

The freight delivery vehicle routing problem cannot be directly applied to an EV fleet, because of additional constraints introduced by EVs such as limited range and charging period requirement [2]. The conventional vehicle routing optimization algorithms should, therefore, be extended taking into account the EV fleet constraints [2, 6]. Further step would be to integrate EV routing and charging optimization, with the final goal to minimize the number of fleet vehicles and/or charging cost. This is a scarce topic of literature with an exception of [55], where both EV routing and charging are considered, although in apparently not (fully) integrated way (also, the charging power limits and RES presence are not considered therein).

Finally, there is a critical aspect of competitiveness of electrified freight transport system when compared to the conventional system. A competitiveness assessment should take into account not only the EV competitiveness (partly addressed in Section 3), but also the charging station investment costs, impact to grid, impact to vehicle routing effectiveness etc. In that sense the reference [56] represents a valuable initial effort on the topic. The overall system design and evaluation can be extended to potentially viable EV fleet system based on battery swapping stations [57, 58], where the EV batteries can be quickly replaced instead of being subject of relatively slow on-vehicle charging.

5 CONCLUSION

The problems of optimal EV architecture design and control and EV optimal charging are strongly dependent on (and linked through) the driving cycle characteristics of a target EV fleet. Therefore, a detailed characterization of fleet behaviors and synthesis of naturalistic driving cycles represent an important aspect of the integrated transport and energy system design, particularly for the freight delivery fleets.

In addition to battery design technologies, the optimized charging management is a key enabling technology for stronger proliferation of electric vehicles and their integration into the power grid. Strong research efforts should be devoted to interactive optimization of EV fleet charging management on the aggregator, individual vehicle distributor, and low-level controller levels. When considering the freight transport, the vehicle routing optimization should be modified to take into account the EV range and charging time constraints, and it should be ultimately integrated with charging optimization.

The assessment of electrified freight transport system competitiveness when compared to the conventional system should take into account different aspects of integrated transport and energy system, such as EV competitiveness, grid impacts, influence on environment in terms of pollution and well-wheel CO2 emission reduction, requirements on charging infrastructure, benefits with respect to proliferation of renewable energy sources, impact on vehicle routing effectiveness and similar.

ACKNOWLEDGMENT

It is gratefully acknowledged that this work has been supported by the Croatian Science Foundation through the project No. 09/128. The data and technical support from Konzum d.d. is gratefully acknowledged, as well.

REFERENCES

[1] J. Shah et al., "Cost-Optimal, Robust Charging of Electrically-Fueled Commercial Vehicle Fleets via Machine Learning", Systems Conference (SysCon), 8th Annual IEEE, Ottawa, ON, Canada, 2014.

[2] J. H. R. van Duin, L. A. Tavasszy and H. J. Quak, "Towards E(lectric)- Urban Freight: First Promising Steps in the Electric Vehicle Revolution", European Transport \Trasporti Europei. vol. 54, no. 9, ISSN 1825-3997, 2013.

[3] H. CityLund and W. Kempton, "Integration of Renewable Energy into the Transport and Electricity Sectors Through V2G", Energy Policy, vol. 36, no. 9, pp. 3578-3587, 2008.

[4] W. Kempton, J. Tomić, "V2G power fundamentals: calculating capacity and net revenue" Journal of Power Sources, vol. 144, no. 1, pp. 268-279, 2005.

[5] R.Garcia-Valle and J. A. Peças Lopes, *Electric Vehicle Integration into Modern Power Networks*, Springer-Verlag New York, 2013.

[6] R. G. Conrad, M. A. Figliozzi, "The Recharging Vehicle Routing Problem", Proceedings of the 2011 Industrial Engineering Research Conference, Reno, Nevada, USA, 2011.

[7] Y. Gao, M. Ehsani, J.M. Miller, "Hybrid Electric Vehicle: Overview and state of the Art", Proc. of IEEE Int. Symp. on Industrial Electronics, pp. 307-315, Dubrovnik, Croatia, 2005.

[8] A. Emadi, *Handbook of Automotive Power Electronics and Motor Drive*, CRC Press, Taylor and Francis Group, 2005.

[9] W. Liu, *Introduction to Hybrid Vehicle System Modeling and Control*, John Wiley & Sons, Inc., Hoboken, NY, USA, 2013.

[10] L. Guzzella, A. Sciarretta, *Vehicle Propulsion Systems - Introduction to Modeling and Optimization*, 2nd ed., Springer-Verlag, Berlin Heidelberg, 2007.

[11] M. Cipek, J. Deur, J. Petrić, "Bond graph modelling and power flow analysis of series–parallel HEV transmissions", International Journal of Powertrains (IJPT), vol. 1, no. 4, pp. 396-419, 2012.

[12] J.M. Miller, "Hybrid Electric Vehicle Propulsion System Architectures of the e-CVT Type", IEEE Transaction on Power Electronic, vol. 21, no. 3, pp. 756-767, 2006.

[13] J.D. Wishart, Y.(L.) Zhou, Z. Dong, "Review, Modelling and Simulation of Two-Mode Hybrid Vehicle Architecture", ASME IDETC/CIE, Las Vegas, Nevada, USA, 2007.

[14] A. Villeneuve, "Dual mode electric infinitely variable transmission", in Proc. SAE TOPTECH Meeting Continuously Variable Transmission, pp. 1-11, 2004.

[15] W. Xiaogang, H. Chen, J. Wang and J. Du, "Energy Efficiency and Economy Analysis of a Range extended Electric Bus in Different Chinese City Driving Cycles", International Journal of u- and e- Service, Science and Technology, vol.7, no.2, 2014.

[16] M.A. Miller, A.G. Holmes, B.M. Conlon and P.J. Savagian, "The GM "Voltec" 4ET50 Multi-Mode Electric Transaxle", SAE paper, no. 2011-01-0887, 2011.

[17] B.M. Conlon, P.J. Savagian, A.G. Holmes and Jr.M.O. Harpster, "Output Split Electrically-Variable Transmission with Electric Propulsion using one or two Motors", U.S. Patent, No. 7 867 124, 2011.

[18] M. Cipek, J. Deur, J. Petrić, "Bond Graph Modeling and Power-flow Analysis of Range Extended Electric Vehicle Transmission", 10th Int. Conference on Bond Graph Modeling & Simulation (ICBGM 2012), Genoa, Italy, 2012.

[19] B. Škugor, M. Cipek and J. Deur, "Control Variables Optimization and Feedback Control Strategy Design for the Blended Operating Regime of an Extended Range Electric Vehicle", SAE International Journal of Alternative Powertrains, SAE paper no. 2014-01-1898, vol. 3, no. 1, pp. 152-162, 2014.

[20] Y. Bin, Y. Li and N. Feng, "Nonlinear dynamic battery model with boundary and scanning hysteresis", Proceedings of the ASME 2009 Dynamic Systems and Control Conference, Hollywood, California, USA, 2009.

[21] M. Cipek, B. Škugor, M. Čorić, J. Kasać and J. Deur, "Control Variable Optimisation for an Extended Range Electric Vehicle", International Journal of Powertrains (IJPT), 2015. (in press)

[22] M. Duoba, R. Carlson, and J. Wu, "Test procedures and benchmarking: Blended-type and EV-capable plug-in hybrid electric vehicles", 23rd International Electric Vehicle Symposium (EVS23), Anaheim, CA, 2007.

[23] L. Tribioli, S. Onori, "Analysis of energy management strategies in plug-in hybrid electric vehicles: Application to the GM Chevrolet Volt", 2013 Proceedings of the American Control Conference, pp. 5966-5971., Washington, DC, USA, 2013.

[24] J. Deur, M. Cipek, B. Škugor, and J. Petrić, Modeling and Low-level Control of Range Extended Electric Vehicle Dynamics, International Conference on Powertrain Modeling and Control (PMC 2012), West Yorkshire, UK, 2012.

[25] Q. Wang, S. Fazal, R. Mcgee, M. Kuang, A. Philips, "Centralized Torque Controller for a Nonminimum Phase Phenomenon in a Powersplit HEV", SAE paper no. 2012-01-1026, 2012.

[26] C. Dextreit and F. Assadian, I.V. Kolmanovsky, J. Mahtani and K. Burnham, "Hybrid Electric Vehicle Energy Management Using Game Theory", SAE paper no. 2008-01-1317, 2008.

[27] M. Duoba, H. Lohse-Busch, R. Carlson, T. Bohn, S. Gurski, "Analysis of Power-Split Control Strategies Using Data from Several Vehicles", SAE paper no.2007-01-0291, 2007.

[28] T. Hofman, M. Steinbuch, R.M. van Druten and A.F.A. Serrarens, "Rule-based equivalent fuel consumption minimisation strategies for hybrid vehicles", 17th IFAC world congress, Seoul, Republic of Korea, 2008.

[29] G. Paganelli, Y. Guezennec and G. Rizzoni, "Optimizing control strategy for hybrid fuel cell vehicle", SAE Paper No. 2002-01-0102, 2002.

[30] C. Musardo, G. Rizzoni and B. Staccia, "A-ECMS: an adaptive algorithm for hybrid electric vehicle energy management", In: 44th IEEE conference on decision and control, and 2005 European control conference, pp. 1816–1823, Seville, Spain, 2005.

[31] B. Škugor, J. Deur, M. Cipek and D. Pavković, "Design of a Power-split Hybrid Electric Vehicle Control System Utilizing a Rule-based Controller and an Equivalent Consumption Minimization Strategy", Proceedings of the Institution of Mechanical Engineers, Part D, Journal of Automobile Engineering, vol. 228, no. 6, pp. 631-648., 2014.

[32] B. Škugor and J. Deur, "Instantaneous Optimization-based Energy Management Control Strategy for Extended Range Electric Vehicle", SAE Paper no. 2013-01-1460, 2013.

[33] T. K. Lee, Z. Filipi, "Synthesis of real-world driving cycles using stochastic process and statistical methodology", Int. J. Vehicle Design, vol. 57, no. 1, pp. 17-36, 2011.

[34] B. Škugor and J. Deur, "The Vehicle Fleet Data Collection, Processing, Analysis, and Naturalistic Driving Cycles Synthesis", 8th Conference on Sustainable Development of Energy, Water and Environment Systems (SDEWES), Dubrovnik, Croatia, 2013.

[35] B. Škugor and J. Deur, "Delivery Vehicle Fleet Data Collection, Analysis, and Naturalistic Driving Cycles Synthesis", Int. J. Innovation and Sustainable Development, Vol. 10, No. 1, 2016.

[36] R. Patil, B. Adornato, Z. Filipi, "Impact of Naturalistic Driving Patterns on PHEV Performance and System Design", SAE paper no. 2009-01-2715, 2009.

[37] ..., http://www.fsb.unizg.hr/acg/syn_natural_driv_cy.html, web page containing the data of synthetic driving cycles

[38] Y. Zou, H. Shi-jie, L. Dong-ge, G. Wei, and X. Hu, "Optimal Energy Control Strategy Design for a Hybrid Electric Vehicle", Discrete Dynamics in Nature and Society, vol. 2013, pp. 1-8, 2013.

[39] MAN Catalogue, TGM 15.240 15 Tonne 4x2 BL Rigid, 2007.

[40] M. Cipek, B. Škugor and J. Deur, "Comparative Characteristics of Conventional and Electric Delivery Vehicles Based on Realistic Driving Cycles", European Electric Vehicle Congress (EEVC 2014), Brussels, Belgium, 2014.

[41] I. J. M. Besselink, P. F. van Oorschot, E. Meinders and H. Nijmeijer, "Design of an Efficient, Low Weight Battery Electric Vehicle Based on a VW Lupo 3L", The 25th World Battery, Hybrid and Fuel Cell Electric Vehicle Symposium & Exhibition (EVS-25), Shenzhen, China, 2010.

[42] EVO Electric Catalogue, AF-230 Motor/Generator, EVO Electric Ltd. 2011.

[43] B. Škugor and J. Deur. "Dynamic Programming-based Optimization of Electric Vehicle Fleet Charging", *IEEE International Electric Vehicle Conference (IEVC)*. Florence, Italy, 2014.

[44] N. Rotering and M. Ilic, "Optimal Charge Control of Plug-In Hybrid Electric Vehicles in Deregulated Electricity Markets", IEEE Transactions on Power Systems, vol. 26, no. 3, pp. 1021-1029, 2011.

[45] O. Sundström and C. Binding, "Flexible Charging Optimization for Electric Vehicles Considering Distribution Grid Constraints", IEEE Transaction on Smart Grid, vol. 3, no. 1, pp. 26-37, 2012.

[46] B. Škugor and J. Deur, "Dynamic Programming-based Optimization of Charging an Electric Vehicle Fleet System Represented by an Aggregate Battery Model", Energy, doi: 10.1016/j.energy.2015.03.057 (*in press*)

[47] M. Gonzalez Vaya and G. Andersson, "Combined Smart-Charging and Frequency Regulation for Fleets of Plug-in Electric Vehicles", IEEE Power and Energy Society General Meeting (PES 2013), Vancouver, BC, Canada, 2013.

[48] M. Yilmaz and P. T. Krein, "Review of Battery Charger Topologies, Charging Power Levels, and Infrastructure for Plug-in Electric and Hybrid Vehicles", IEEE Transactions on Power Electronics, vol. 28, no. 5, pp. 2151 – 2169, 2013.

[49] M. Yilmaz and P. T. Krein, "Review of the Impact of Vehicle-to-Grid Technologies on Distribution Systems and Utility Interfaces", IEEE Transactions on Power Electronics, vol. 28, no. 12, pp. 5673 – 5689, 2013.

[50] J. Gallardo-Lozano, E. Romero-Cadaval, V. Mińambres-Marcos, D. Vinnikov, T. Jalakas and H. Hőimoja, "Grid Reactive Power Compensation by Using Electric Vehicles", In Proc. of IEEE 2014 Electric Power Quality and Supply Reliability Conference, Rakvere, Estonia, pp. 19-24, 2014.

[51] M. Kesler, M. C. Kisacikoglu and L. M. Tolbert, "Vehicle-to-Grid Reactive Power Operation Using Plug-In Electric Vehicle Bidirectional Offboard Charger", IEEE Transactions on Industrial Electronics, vol. 61, no. 12, pp. 6778 - 6784, 2014.

[52] M. C. Kisacikoglu, B. Ozpineci and L. M. Tolbert, "EV/PHEV Bidirectional Charger Assessment for V2G Reactive Power Operation", IEEE Transactions on Power Electronics, vol. 28, no. 12, pp. 5717 – 5727, 2013.

[53] B. Škugor and J. Deur, "A Novel Model of Electric Vehicle Fleet Aggregate Battery for Energy Planning Studies", Energy, doi:10.1016/j.energy.2015.05.030 (in press)

[54] M. Montazeri-Gh, A. Fotouhi, and A. Naderpour, "Driving patterns clustering based on driving features analysis", Proceedings of the Institution of Mechanical Engineers, Part C: Journal of Mechanical Engineering Science, vol. 225, no.6, pp. 1301-1317, 2011.

[55] J. Barco, A. Guerra, L. Muńoz and N. Quijano, "Optimal Routing and Scheduling of Charge for Electric Vehicles: Case Study", 2013.

[56] B. A. Davis and M. A. Figliozzi, “A Methodology to Evaluate the Competitiveness of Electric Delivery Trucks”, Transportation Research Part E, vol. 49, no. 1, pp. 8–23, 2013.

[57] M. Armstrong, C. El Hajj Moussa, J. Adnot, A. Galli and P. Riviere, “Optimal Recharging Strategy for Battery-Switch Stations for Electric Vehicles in France”, Energy Policy, vol. 60, pp. 569–582, 2013.

[58] O. Worley and D. Klabjan, “Optimization of Battery Charging and Purchasing at Electric Vehicle Battery Swap Stations”, IEEE Vehicle Power and Propulsion Conference (VPPC), 2011.

Joško Deur is a Full Professor at the University of Zagreb, where he teaches courses in electrical machines and servodrives, digital control systems, and automotive mechatronics. In 2000, he spent a year with the Ford Research Laboratory, Dearborn, MI, as a postdoctoral scholar. Professor Deur has led numerous projects including those supported by Ford Motor Company and Jaguar Cars Ltd. His main research interests include modelling and control of automotive systems including electrical vehicles, and control of electrical servo-drives.

Branimir Škugor is a Research Assistant at the University of Zagreb. He was a Ph.D. student on the project entitled "ICT-aided integration of Electric Vehicles into the Energy Systems with a high share of Renewable Energy Sources" and supported by the Croatian Science Foundation. His research interests include hybrid electric vehicle controls, smart charging, optimisation algorithms, and probability analyses.

Mihael Cipek is a Research and Teaching Assistant at the University of Zagreb, Croatia. He received his PhD in Mechanical Engineering from the University of Zagreb in 2015. The field of his research interest is modelling and control of automotive mechatronic systems.

AUTHORS' ADDRESSES

Prof. Joško Deur, Ph.D.
Branimir Škugor, M. Sc.
Mihael Cipek, Ph. D.
Department of Robotics and Automation of Manufacturing Systems,
Faculty of Mechanical Engineering and Naval Architecture, University of Zagreb,
I. Lučića 5, HR-10002, Zagreb, Croatia
email: josko.deur@fsb.hr, branimir.skugor@fsb.hr.hr, mihael.cipek@fsb.hr

Received: 2014-11-21
Accepted: 2015-04-15